Acta Cryst. (1998). B**54**, 345–350

Structural Determination of the Hydrofullerene $C_{60}D_{36}$ by Neutron Diffraction

L. E. HALL,[a] D. R. MCKENZIE,[a]* R. L. DAVIS,[b] M. I. ATTALLA[c] AND A. M. VASSALLO[c]

[a]*School of Physics, University of Sydney, NSW 2006, Australia,* [b]*Late of Australian Institute of Nuclear Science and Engineering, Private Mail Bag 1 Menai, VSW 2234, Australia, and* [c]*CSIRO Division of Coal and Energy Technology, PO Box 136, North Ryde, NSW 2113, Australia. E-mail: mckenzie@physics.usyd.edu.au*

(*Received 9 September 1997; accepted 20 December 1997*)

Abstract

A mixture of $C_{60}D_{36}$ with 24.5 ± 4.5% C_{60} by weight has been analysed by neutron diffraction techniques. The diffraction data was converted to a reduced density function $G(r)$ by Fourier transformation. The C_{60} component of the $G(r)$ was subtracted out. This enabled a comparison for five molecular models of $C_{60}D_{36}$, with symmetries T, T_h, S_6 and two D_{3d} isomers, with the experimental $G(r)$. This specimen of $C_{60}D_{36}$ was found to be best described by a T symmetry isomer, in agreement with ^{13}C NMR and IR data for $C_{60}H_{36}$ [Attalla *et al.* (1993). *J. Phys. Chem.* pp. 6329–6331].

1. Introduction

The molecule $C_{60}H_{36}$, a hydrogenated derivative of the fullerene C_{60}, has recently been prepared using high-pressure hydrogenation (Attalla *et al.*, 1993). The aim of this work was to study the molecular structure and packing of $C_{60}H_{36}$ and its deuterated equivalent, $C_{60}D_{36}$, in the solid state. Initially it was assumed that the $C_{60}H_{36}$ molecule exists only as a single isomer. This issue was then reexamined in the light of the agreement with experiment.

The hydrogenation of 36 C atoms in the C_{60} truncated icosahedron necessarily lowers the symmetry of the original molecule, because of the local distortion resulting from the sp^3 rather than sp^2 hybridization of protonated carbons. As is the case with C_{60} itself, dynamic or static disorder limits the use of conventional single-crystal X-ray crystallographic techniques for the determination of the internal molecular structure. Accordingly, we have used a method based on the Fourier transform of the intensity which enables us to work in real space with a reduced density function which we fit to a model. The reduced density method has previously been used for determining the internal structure of the C_{70} molecule from electron diffraction data (McKenzie *et al.*, 1992) and the structure of C_{60} using neutron diffraction data (Li *et al.*, 1991). The real space approach is effective in such cases, since the effect of large molecular orientational disorder is to remove unwanted information concerning intermolecular distances, leaving only intramolecular information. We show that even in the presence of correlations between the orientations of molecules in neighbouring cells the intramolecular information dominates the $G(r)$. Since the intramolecular distances dominate, the reduced density function is sensitive to the molecular structure and can be readily fitted with a molecular model. In this study we use neutron diffraction since electron and X-ray diffraction are not sensitive to the positions of the H atoms relative to the carbon cage. Neutron diffraction, on the other hand, provides an opportunity to study the hydrogen positions, especially in the case of the deuterated molecule, since deuterium scatters neutrons as strongly as carbon. The respective scattering lengths for carbon, deuterium and hydrogen are 0.6648, 0.6672 and −0.3617. Hydrogen also has the disadvantage of a large incoherent scattering cross section.

2. Sample preparation

The deuterated fullerene ($C_{60}D_{36}$) was prepared by the high-pressure reduction technique reported by Attalla *et al.* (1993). Pure C_{60} was obtained from MER Corporation and the stated level of purity was 99.5%. It was used without further purification. All other reagents were of analytical grade. In a typical preparation, C_{60} (500 mg) was placed in a glass vessel inside a Parr autoclave (250 cm^3) with iodine (1.5 g) and the vessel pressurized with deuterium to 3.4 MPa (500 p.s.i.) cold charge. The autoclave was heated to 623 K and maintained at that temperature for 1 h. After cooling, the product was removed and washed with aqueous $Na_2S_2O_3$ (25% wt/wt, 75 cm^3) to remove residual iodine and then with excess water.

^{13}C solid-state NMR spectra were acquired on a Bruker CXP-90 instrument at ambient temperatures, operating at the frequency 22.36 MHz. The spectra represent single pulse experiments without decoupling during the data acquisition stage and with magic angle spinning at 4 kHz. A ^{13}C pulse time of 3.5 ms was used in conjunction with a recycle delay of 180 s. All ^{13}C chemical shifts are externally referenced to TMS. The pale yellowish–brown powder obtained contained by weight 75.5% $C_{60}D_{36}$ and 24.5 ± 4.5% C_{60}.

3. Neutron diffraction

Data were collected on the SANDALS spectrometer on the ISIS spallation neutron source at the Rutherford–Appleton Laboratory, which has a resolution of approximately 2% of s (Nikolaev *et al.*, 1993). The powder specimen of 75.5% $C_{60}D_{36}$ and 24.5% C_{60}, weighing 0.5 g, was mounted in a vanadium can. The experimental data were collected at 4.2 K and at ambient temperature (294 K) to the s range $0.02 < s < 4$ Å^{-1}, where $s = Q/2\pi$. The background from the vanadium was extracted and corrections due to multiple scattering were performed according to the procedures of Soper (1994). The raw intensity $I(s)$ was converted to a reduced intensity function defined by

$$\varphi(s) = s(I(s) - N\langle f^2\rangle)/N\langle f\rangle^2, \quad (1)$$

where $\langle f^2\rangle = X_C f_C^2 + X_D f_D^2$ and $\langle f\rangle^2 = (X_C f_C + X_D f_D)^2$ (X_C and X_D are the atomic fractions), N is a scaling factor, and f_C and f_D are the elastic scattering lengths for carbon and deuterium, respectively. Fig. 1 shows the reduced intensity of polycrystalline $C_{60}D_{36}$ at room temperature and 4.3 K for $0.02 < s < 4.0$ Å^{-1}, while Fig. 2 shows the region $0.02 < s < 0.5$ Å^{-1}.

The room-temperature peak positions up to s = 0.4 Å^{-1} were well fitted by a body-centred cubic (b.c.c.) lattice model with a cubic cell dimension of 11.8 ± 0.1 Å, see Table 1. This is in good agreement with the value 11.785 ± 0.015 Å obtained from X-ray diffraction data (Hall *et al.*, 1993), indicating that the presence of 24.5% C_{60} has not significantly altered the crystalline structure of $C_{60}H_{36}$ with 10–15% of $C_{70}H_{36}$ from the structure of Hall *et al.* (1993). From Fig. 2 and Table 1 it can be seen that the b.c.c. lattice is maintained at 4.2 K with a cell dimension of 11.6 ± 0.1 Å.

A pure C_{60} sample has a face-centred cubic (f.c.c.) structure with a lattice constant of 14.2 Å (Fleming *et al.*, 1991). Diffraction peaks should therefore occur at s = 0.122, 0.199, 0.234, 0.244, 0.307, 0.315, 0.345 and 0.366 Å^{-1}. The peak positions of s = 0.345 and 0.366 Å^{-1} are distinguishable from the b.c.c. peak positions and cannot be detected, as seen in Fig. 2. With such a large percentage of C_{60} present in the mixture, the absence of a separate C_{60} phase shows that the C_{60} molecules of the material are well mixed in with the b.c.c. $C_{60}D_{36}$ phase and there is no detectable separated f.c.c. C_{60} phase.

Table 1. *Comparison between the experimental neutron diffraction peak positions (±.003 Å^{-1}) of $C_{60}D_{36}$ with 24.5% of C_{60}, and the fitted b.c.c. indexed peak positions (accurate to last significant figure), in units of s at 294 and 4.2 K, respectively*

294 K, a = 11.8 Å		4.2 K, a = 11.6 Å	
Experimental	Calculated	Experimental	Calculated
0.120	0.120	0.121	0.122
0.169	0.169	0.171	0.172
0.207	0.207	0.209	0.211
0.235	0.239	0.240	0.244
0.293	0.293	0.298	0.299
0.316	0.317	0.321	0.323
0.398	0.397	0.404	0.404
0.414	0.415	0.421	0.422

3.1. *Method of structural analysis*

The reduced intensity function can be converted to the reduced density function $G(r)$ by Fourier transformation

$$G(r) = 8\pi \int s\varphi(s)\sin(2\pi sr)\mathrm{d}s$$
$$= 4\pi r(\rho(r) - \rho_0), \quad (2)$$

where $\rho(r)$ is the spherically averaged atomic density and ρ_0 is the average atomic density. Peaks in $G(r)$ correspond to interatomic distances.

3.1.1. *Broadening of the intramolecular reduced density function.* There are two types of thermal vibrational modes that are weakly coupled to each

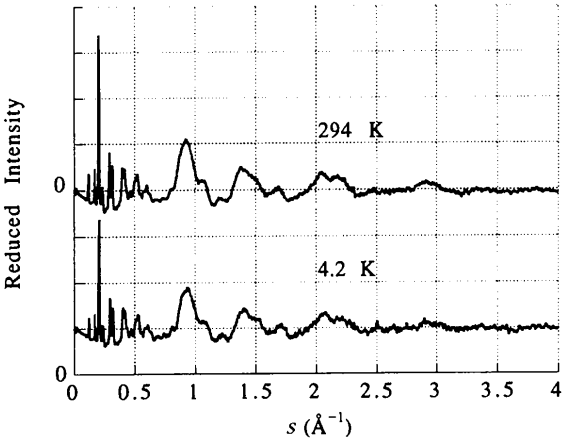

Fig. 1. Reduced intensity function for room temperature and 4.2 K mixture of 75.5% $C_{60}D_{36}$ and 24.5% C_{60}.

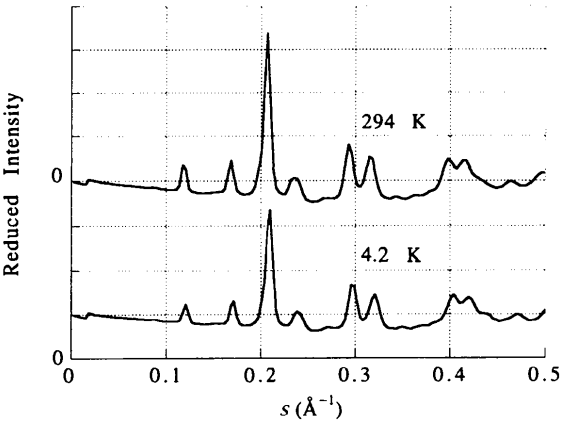

Fig. 2. Enlargement of Fig. 1 at small s, showing the intermolecular diffraction peaks at 294 and 4.2 K.

other: the intramolecular modes of vibration and the vibrational modes of the molecule as a whole. In addition to thermal effects there are static disorder effects. The combined effect of all these phenomena averaged over a large number of 'snapshots' is simply to give a distribution of bond lengths. This can be modelled by convoluting each distance with a Gaussian, as outlined by Nikolaev *et al.* (1993) and Soper *et al.* (1992) for C_{70}. These authors used a model which convolved each intramolecular distance with a Gaussian function whose width is given by $\sigma_1 + \sigma_2(r_{ij})^{1/2}$. They found the value of σ_1 was 0.05–0.06 Å and σ_2 = 0.32 Å for C_{70}. The atomic displacements due to the zero-point motion found by Onida *et al.* (1994) for C_{70} was approximately 0.07 Å, in agreement with the value of 0.05–0.06 Å found by Nikolaev *et al.* (1993). The distance-dependent broadening arises from the intramolecular modes and is in contrast to the broadening that occurs in monoatomic crystalline materials whose temperature broadening effects are typically modelled by a Gaussian of constant width, independent of the interatomic distance. In our case each contributing peak to the $G(r)$ then needs to be convolved by a Gaussian to take into account the temperature effects.

3.2. *Intermolecular correlation, small-angle scattering and C_{60} impurity effects*

There are three effects which can modify the reduced density function of a molecule in a crystallite from its form for an isolated $C_{60}D_{36}$ molecule. The first is the truncation of the data at small scattering angles, the second is the effect of orientational correlation between molecules in adjacent cells and the third is the presence of C_{60} as a contamination. These effects can be quantified by calculation of the diffracted intensity and subsequently the $G(r)$, from a spherical crystallite containing 729 molecules. A D_{3d} isomer of $C_{60}D_{36}$ was chosen as a test case using the coordinates of Hall *et al.* (1993). The effect of intermolecular correlations was simulated by imposing a partial orientational ordering, in which the distances between D atoms was maximized and the molecules were allowed to librate by an average of 3° away from this orientation in every direction. This small libration amplitude will underestimate the effect of intermolecular correlations, since at room temperature the libration amplitude is likely to be larger than this. The effect of C_{60} contamination was modelled by replacing 179 of the 729 molecules by C_{60} using the coordinates of Li *et al.* (1991).

The $G(r)$ of the crystallite was calculated from the calculated diffracted intensity after processing data within $0.6 < s < 4.0$ Å^{-1} and subtracting the effect of C_{60} using the following formula

$$G_{C_{60}D_{36}}(r) = [(96 - 36x)G_{mix}(r) - 60xG_{C_{60}}(r)]/(96[1 - x]). \quad (3)$$

The final result for $G(r)$ is compared in Fig. 3 with the result for a single molecule. The good agreement justifies our neglect of small-angle scattering, neglect of intermolecular correlation and the subtraction of the C_{60} impurity effects.

4. Comparison of experimental and theoretically calculated $G(r)$ models of $C_{60}D_{36}$

The experimentally determined $G(r)$ was compared with the $G(r)$ calculated for five different molecular structures, as shown in Fig. 4. An appropriate 'goodness-of-fit' factor is defined by (4) (Nikolaev *et al.*, 1993)

$$R_f = \{[\Sigma w(r)(G_{exp}(r) - G_{calc}(r))^2]/[\Sigma w(r)(G_{exp}(r))^2]\}^{1/2}, \quad (4)$$

where $w(r)$ is a weighting function, typically $r^{-0.5}$. The

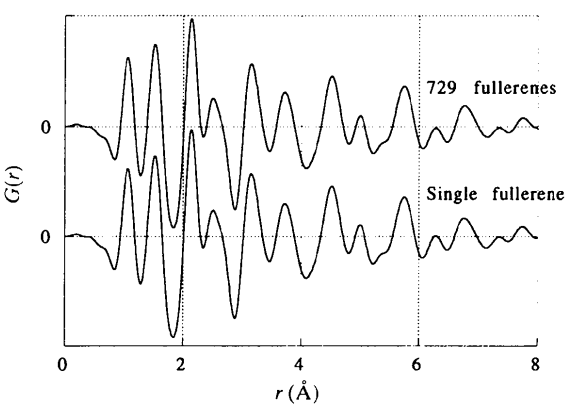

Fig. 3. Comparison of $G(r)$ for a single $C_{60}D_{36}$ molecule to that of a 729 fullerene mixture after the C_{60} impurity had been subtracted out.

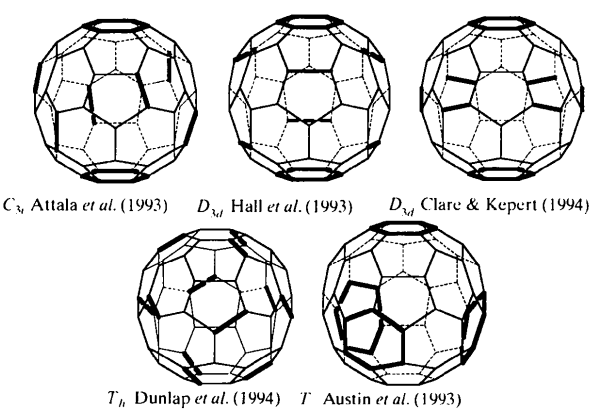

Fig. 4. Structures of $C_{60}H_{36}$ molecules. The highlighted bonds correspond to the bonds between unhydrogenated C atoms.

molecular structure given by Dunlap *et al.* (1991) has T_h symmetry. These authors obtained their molecular coordinates using density functional theory with a Perdew–Zunger (Perdew & Zunger, 1981) fit to the free electron gas results of Ceperley & Alder (1980). The C_{3i} structure was calculated using semi-empirical techniques (MNDO carried out on a CRAY computer using the UniChem package; Attalla *et al.*, 1993).

The coordinates of the proposed D_{3d} model (Hall *et al.*, 1993) were estimated by setting the C—H bond lengths to 1.10 Å, the double-bond lengths to 1.33 Å, the sp^3—sp^3 C bonds to 1.58 Å and all other bond lengths to 1.46 Å. These coordinates were then relaxed from the initial hypothetical structure into a lower energy configuration using the semi-empirical technique *MNDO* (Attalla, 1995). The coordinates for the isomer of T symmetry (Austin *et al.*, 1993) and the second isomer of D_{3d} symmetry of Clare & Kepert (1994) were calculated using the empirical AM1 Hamiltonian. In Fig. 4 the bonds between unhydrogenated C atoms are highlighted. In the T_h isomer these bonds are maximally separated from each other. The C_3 axis can be clearly seen for the C_{3i} and the two D_{3d} models. The tetrahedral symmetry of the T model is shown by the positions of the four unhydrogenated hexagons.

From the coordinates of the five different molecular structures, the $G(r)$ values were calculated using the method outlined by Hall & Marks (1998), which takes into account thermal vibrations and the effects of s-dependent instrumental broadening. The resulting calculated $G(r)$ curves were then compared with the $G(r)$ measured at room temperature, as shown in Fig. 5. The room-temperature $G(r)$ was used in preference to the low-temperature data in order to minimize the effect of intermolecular correlations.

In order to rank the proposed structures in order of their agreement with experiment, the R factor, shown in (4), was evaluated for each model using a weighting function $w(r)$ used with the weighting function $r^{-0.5}$.

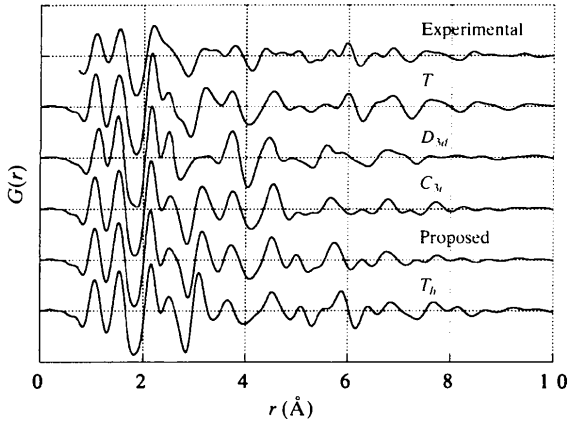

Fig. 5. Comparison of the predicted and experimental $G(r)$ of $C_{60}D_{36}$.

Table 2. *The R factor for each of the predicted $C_{60}D_{36}$ G(r) functions from the experimental G(r) function*

Model	Symmetry	R factor
Austin *et al.* (1993)	T	0.3513
Attalla *et al.* (1993)	C_{3i}	0.4680
Clare & Kepert (1994)	D_{3d}	0.4767
Proposed (Hall *et al.*, 1993)	D_{3d}	0.5190
Dunlap *et al.* (1991)	T_h	0.5415

Table 2 shows that the model having the best agreement with the experimental $G(r)$ is clearly the T symmetry model of Austin *et al.* (1993).

Although the agreement between the T symmetry model to the experimental data is the best of the models examined, there are regions within the $G(r)$ where differences are still apparent. The peaks at 2.0–2.5 Å of the experimental $G(r)$ are more diffuse, and at 3.1 and 4.5 Å there are double peaks as opposed to the single peaks of the T symmetry molecule. To further refine the fit between the predicted and experimental $G(r)$, the theoretically calculated symmetry-inequivalent coordinates were used as input for the computer code. The function $T(r)$ defined as

$$T(r) = G(r) + 4\pi r\rho_0 \qquad (5)$$

for a set of individual distances from 1.0 to 11.0 Å in increments of 0.002 Å was calculated. The intramolecular distances were calculated for the initial model and rounded off to the nearest 0.002 Å. The $s\varphi(s)$ was calculated up to 0.6 $Å^{-1}$ and Fourier transformed. The Fourier transform of the $s\varphi(s)$ was subtracted from the total $T(r)$ to give the $G(r)$. The function that was subtracted from the $T(r)$ was held constant unless the symmetry-inequivalent coordinates moved by more than 0.02 Å. Whenever a symmetry-inequivalent atom was moved, the individual $T(r)$ peaks were subtracted from the $G(r)$ and the new $T(r)$ peaks were added to it, giving the new $G(r)$. It was found that this method was more computationally efficient than the method which simply Fourier transforms the total $s\varphi(s)$.

4.1. *Relaxation of molecular models*

The symmetry-inequivalent atoms for each of the $C_{60}D_{36}$ symmetry models were moved until further adjustments did not improve the fit to the experimental $G(r)$. Fig. 6 shows the $G(r)$ of all the relaxed models with the experimental $G(r)$. The improvement of each relaxed $G(r)$ model with the experimental $G(r)$ can be seen by comparing it with Fig. 5. The R factors shown in Table 3 indicate that the best model is again clearly the T symmetry model with all other models showing similar R factors, except for the D_{3d} model of Clare & Kepert (1994). This is a little surprising as Clare & Kepert (1994) found that both the T and D_{3d} model have very similar energies. However, from Fig. 6 the

Table 3. *The R factor for each of the predicted $C_{60}D_{36}$ G(r) functions from the experimental G(r) function*

Model	Symmetry	R factor
Austin *et al.* (1993)	T	0.2170
Proposed	D_{3d}	0.3227
Attalla *et al.* (1993)	C_{3i}	0.3240
Dunlap *et al.* (1991)	T_h	0.3361
Clare & Kepert (1994)	D_{3d}	0.3994

relaxed D_{3d} model of Clare & Kepert (1994) can be seen to have several regions of strong disagreement with the experimental $G(r)$. It must be noted that compared with the R factors calculated by Nikolaev *et al.* (1993), who fitted a calculated $I(s)$ to the experimental $I(s)$ for C_{70}, these R factors are relatively large. This is because the $G(r)$ oscillate through zero as opposed to the $I(s)$ curves which oscillate around a constant. Referring to (4), the $G(r)$ method then has a significantly smaller denominator, giving a much larger R factor. The pair correlation function defined as

$$g(r) = [G(r)/(4\pi r\rho_{avg})] + 1 \qquad (6)$$

could have been used, giving significantly smaller R factors, for example, the relaxed T symmetry model gives an R factor of 0.04. However, this function weights the peaks at small r considerably and as all models have very similar first and second peak distances and heights then these R factors will not discriminate between models clearly. It is only for $r > 2$ Å that the $G(r)$ curves behave very differently and it is here where any obvious disagreement with the experimental $G(r)$ can be detected.

On examination of the relaxed coordinates of the T symmetry model two changes have occurred. The first is that the carbon–hydrogen bond lengths have increased from an average length of 1.074 to 1.105 Å. The second is that the two longest carbon–carbon bond lengths of 1.627 and 1.594 Å have decreased to 1.610 and 1.566 Å, respectively. Bond angles did not change significantly;

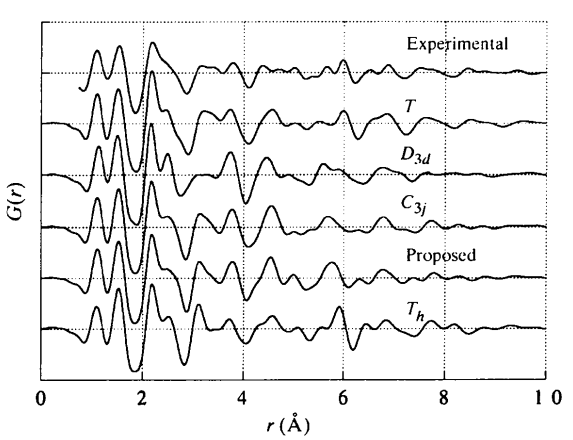

Fig. 6. Comparison of the relaxed and experimental $G(r)$ of $C_{60}D_{36}$.

Table 4. *Symmetry-inequivalent coordinates for the relaxed T model, error ±0.02, compared with the coordinates of Dunlap et al. (1994)*

	Initial			Relaxed	
Carbon					
x	y	z	x	y	z
2.334	−0.491	2.041	2.33	−0.49	2.04
2.758	−1.205	0.927	2.76	−1.20	0.93
3.855	−0.783	−0.026	3.84	−0.78	−0.04
2.873	−0.842	−2.524	2.85	−0.85	−2.52
2.440	−1.663	−1.330	3.43	−1.67	−1.33
Hydrogen					
4.854	−1.086	0.213	4.86	−1.09	0.23
−3.714	0.756	−3.188	−3.72	0.75	−3.18
−4.358	2.097	−1.690	−4.38	2.10	−1.69

the greatest change was for a C—C—D angle of 117.2 to 114.8°, a decrease of 2.4°. Table 4 shows the relaxed symmetry-inequivalent coordinates compared with the initial coordinates of Dunlap *et al.* (1994). The errors in the relaxed coordinates are due to the uncertainty of the concentration of the C_{60} impurity within the sample of $C_{60}D_{36}$. However, on varying the impurity level between the two examples the T symmetry model always has the better fit to the experimental $G(r)$, with all R factors varying by at most 0.03.

A residual disagreement between the experimental and the relaxed theoretical $G(r)$ of the T symmetry molecule still exists and could arise from distortions caused by the location of the molecule in a crystal lattice or from the presence of other isomers.

5. Mixture of isomers

The $G(r)$ for a mixture of isomers can be expressed as $aG(r)_1 + bG(r)_2 + \cdots$, where a is the percentage of isomer 1, b is the percentage of isomer 2 *etc.* The R factor was minimized for a combination of all the five above-mentioned isomers by varying the constants a, b *etc.* The R factor was found to increase upon mixing the T symmetry model with any combination of the other models. This indicates that if any of the other isomers coexist with the T symmetry model, then it must exist in small amounts.

6. Discussion and conclusions

The T symmetry model has the unique feature of four unhydrogenated benzene rings. This is ideal for the b.c.c. packing of the molecules as the unsaturated benzene rings can face in the [111] directions, which will then be facing the saturated hexagonal rings of the neighbouring molecules, which will face the $[\bar{1}\bar{1}\bar{1}]$ directions. With this orientation the minimum distance between atoms of neighbouring molecules is the largest of the isomers examined. All the other isomers inves-

tigated above do not have this characteristic of having hydrogen-deficient regions 109.47° apart.

The intermolecular packing of 75.5% $C_{60}H_{36}$ with 24.5% C_{60} was confirmed to be body-centred cubic with a cell dimension of 11.8 ± 0.1 Å at room temperature and 11.6 ± 0.1 Å at 4.2 K. The molecular structure that provides the best agreement with experimental data for $C_{60}H_{36}$, at room temperature and 4.2 K, is the relatively low-symmetry T structure predicted by Austin *et al.* (1993). The agreement between the experimental $G(r)$ with this structure was considerably improved by moving the D-atom positions while retaining the symmetry. The $G(r)$ method cannot determine whether there are any other isomers coexisting with the T symmetry molecule, but suggests that they could occur at most in small concentrations. The dominant error in the relaxed coordinates of the T symmetry model arises from the uncertainty of the C_{60} impurity within the sample.

References

Attalla, M. I. (1995). Personal communication.

Attalla, M. I., Vassallo, A. M., Tattum, B. & Hanna, J. V. (1993). *J. Phys. Chem.* pp. 6329–6331.

Austin, S. J., Batten, R. C., Fowler, P. W., Redmond, D. B. & Taylor, R. (1993). *J. Chem. Soc. Perkin Trans. 2*, pp. 1383–1386.

Ceperley, D. M. & Alder, B. J. (1980). *Phys. Rev. Lett.* **45**, 566–569.

Clare, B. W. & Kepert, D. L. (1994). *J. Mol. Struct.* **304**, 181–189.

Dunlap, B. I., Brenner, D. W., Mintmire, J. W., Mowrey, R. C. & White, C. T. (1991). *J. Phys. Chem.* **95**, 5763–5768.

Dunlap, B. I., Brenner, D. W. & Schriver, G. W. (1994). *J. Phys. Chem.* **98**, 1756–1757.

Fleming, R. M., Siegrist, T., Marsh, P., Hessen, B., Kortan, A. R., Murphy, D. W., Haddon, R. C., Tycko, R., Cabbagh, G., Mujsce, A. M., Kaplan, M. L. & Zahurak, S. M. (1991). *Mater. Res. Soc. Symp. Proc.* MRS Conference, Pittsburgh. Materials Research Society.

Hall, L. E. & Marks, N. A. (1998). In preparation.

Hall, L. E., McKenzie, D. R., Attalla, M. I., Vassallo, A. M., Davis, R. L., Dunlop, J. B. & Cockayne, D. J. H. (1993). *J. Phys. Chem.* **97**, 5741–5744.

Li, F., Ramage, D., Lannin, J. K. & Conceicao, J. (1991). *Phys. Rev. B*, **44**, 13167–13170.

McKenzie, D. R., Davis, C. A., Cockayne, D. J. H., Muller, D. A. & Vassallo, A. M. (1992). *Nature (London)*, **355**, 622–624.

Nikolaev, A. V., Dennis, T. J. S., Prassides, K. & Soper, A. K. (1993). *Chem. Phys. Lett.* **223**, 143–148.

Onida, G., Andreoni, W., Kohanoff, J. & Parrinello, M. (1994). *Chem. Phys. Lett.* **219**, 1–7.

Perdew, J. P. & Zunger, A. (1981). *Phys. Rev. B*, **23**, 5948–5951.

Soper, A. K. (1994). Personal communication.

Soper, A. K., David, W. I. F., Sivia, D. S., Dennis, T. J. S., Hare, J. P. & Prassides, K. (1992). *J. Phys. Condens. Matter*, **4**, 6087–6094.